

ENGINEERING DIVISION
U.S. ARMY ENGINEER REACTORS GROUP
CORPS OF ENGINEERS
FT BELVOIR, VA. 22060

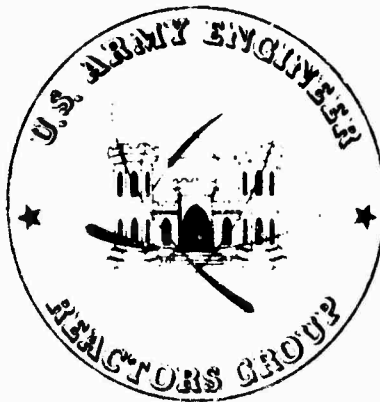
AD

AD707453

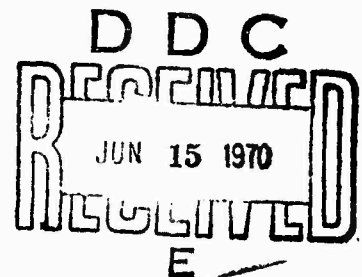
ED-7002
MH-1A Core Physics Test Report

C. FREDERICK SEARS, CPT, C.E.
MICHAEL V. GREGORY, PFC

MARCH 16, 1970



Reproduced by the
CLEARINGHOUSE
for Federal Scientific & Technical
Information Springfield Va 22151

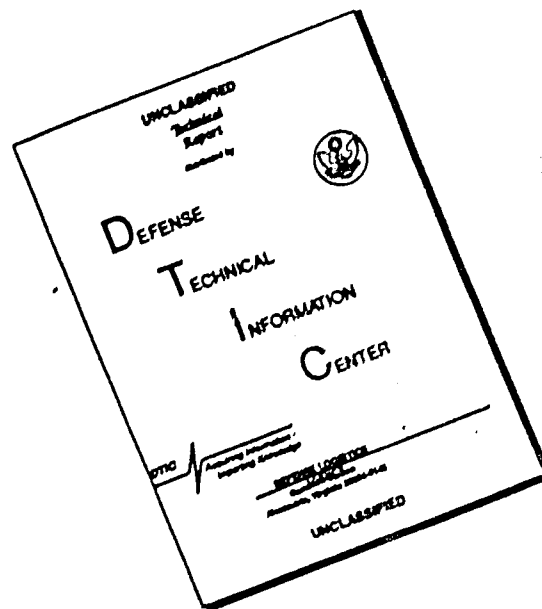


Distribution of this document is unlimited.

This document has been approved
for public release and sale; its
distribution is unlimited

46

DISCLAIMER NOTICE



THIS DOCUMENT IS BEST QUALITY AVAILABLE. THE COPY FURNISHED TO DTIC CONTAINED A SIGNIFICANT NUMBER OF PAGES WHICH DO NOT REPRODUCE LEGIBLY.

ACCESSION NO.	
APSTI	WHITE SPOTING <input checked="" type="checkbox"/>
BDC	DIFF. TESTING <input type="checkbox"/>
CHAMPIONED	<input type="checkbox"/>
JUSTIFICATION	
BY	
DISTRIBUTION/AVAILABILITY CODES	
DECL.	AVAIL. and/or SPECIAL
/	

The findings in this report are not to be construed as an official Department of the Army position, unless so designated by other authorized documents.

Destroy this report when it no longer needed. Do not return it to the originator.

ED-7002
MH-1A CORE PHYSICS TEST REPORT

C. FREDERICK SEARS, CPT, C.E.
MICHAEL V. GREGORY, PFC

MARCH 16, 1970

ENGINEERING DIVISION
U. S. ARMY ENGINEER REACTORS GROUP
CORPS OF ENGINEERS

ABSTRACT

Core physics measurements were performed in November 1969 on the first refueled core of the MH-1A (Sturgis). This report presents and analyzes the data recorded. The basic physical parameters describing the core are derived and compared with the pre-refueling values and the theoretical values.

TABLE OF CONTENTS

Title	Page
I Introduction	1
II Discussion	1
A. Initial Approach to Criticality	1
B. Stuck Rod Shutdown Margin Test	2
C. Control Rod Calibrations	6
D. Temperature Coefficient of Reactivity	21
E. Power Coefficient of Reactivity	29
F. Equilibrium Xenon	31
III Conclusions	37

LIST OF TABLES

Title	Page
I Initial Approach to Criticality	1-2
II Stuck Rod Shutdown Margin Measurements	4
III Fully Withdrawn Integral Rod Worths	7
IV Control Rod #1 Calibration at 147°F, 320 psig	13-14
V Control Rod #1 Calibration at 485°F, 1355 psig	15-16
VI Control Rod #12 Calibration at 147°F, 320 psig	17-18
VII Control Rod #12 Calibration at 489°F, 1360 psig	19-20
VIII Temperature Coefficient	23
IX Temperature Coefficient (11 Nov 69)	25-26
X Temperature Coefficient (15 Nov 69)	27-28-29
XI Power Coefficient Data	31-32
XII Summary Comparison	39

LIST OF FIGURES

Title	Page
1 Initial Approach to Criticality	3
2 Core-Detector Orientation	5
3 Control Rod #1 Integral Worth Curves	8
3a Control Rod #1 Differential Worth Curve	9
3b Control Rod #1 Differential Worth Curve	10
4 Control Rod #12 Integral Worth Curves	11
4a Control Rod #12 Differential Worth Curves	12
5 Temperature Coefficient Data	22
6 Quadratic Curve Fit to Temp. Coefficient Data	24
7 Power Coefficient Data	30
8 Extrapolation to Obtain Missing Data	33
9 Xenon Build-Up (Experimental Data)	35
10 Xenon Build-Up (Corrected Data)	38
References	40

I. INTRODUCTION

Core physics measurements were performed on the refueled MH-1A core in November 1969. The results are analyzed herein. Those parameters which are important in understanding core behavior (such as the temperature and power coefficients of reactivity, rod worths, xenon build-up, critical bank position) are derived from the data. Comparisons are made with expected values for these quantities.

II. DISCUSSION

A. Initial Approach to Criticality

The initial approach to criticality after the first refueling of the MH-1A (STURGIS) was conducted on 11 November 1969. Table I gives the data for the approach and Figure I gives the inverse multiplication curve. The curves for both channels predicted a critical bank of 11.5⁺ inches withdrawal. The measured critical bank was 11.48 inches. This was at a temperature of 150°F and a pressure of 320 psig.

During a two-decade power rise after achieving criticality, a period of 87.3 seconds for a 12 rod bank of 11.53 inches withdrawal was observed. This corresponds to a positive reactivity of 10.3 c or about \$2.06 per inch differential bank worth at 11.5 inches.

The rod latch check was performed using the reactivity computer. All twelve rods were found to be latched. Verification of rod movement required less than .5 inch insertion of each rod to produce an observable negative reactivity.

TABLE I

Initial Approach to Criticality

12 Rod Bank Position (inches)	Source Range Channel 1 (cpm)	Source Range Channel 2 (cpm)
0.03	1245	1237
2.00	1297	1231
4.00	1361	1356
6.00	1516	1429
8.00	2102	2142

TABLE I (continued)

Initial Approach to Criticality

12 Rod Bank Position (inches)	Source Range Channel 1 (cpm)	Source Range Channel 2 (cpm)
9.00	3031	2834
10.00	5087	4660
10.50	7398	7289
11.00	14496	13715

B. Stuck Rod Shutdown Margin Test

The stuck rod shutdown margin test was performed on 11 November 1969. Two inner rods and three outer rods were evaluated in this test (Table II). The critical eleven rod bank positions for the simulated stuck rods indicate the inner rods have similar shutdown margins, and the outer rods have similar shutdown margins. It was therefore not necessary to measure the shutdown margin for each rod but only for representative ones.

The critical eleven rod bank for an outer stuck rod was slightly higher than that for an inner rod. The shutdown margin measurements for an inner rod (#1) and an outer rod (#5) indicated however, that an inner rod had a significantly greater margin than did the outer rod. See Figure 2 for the core layout. Since the eleven rod critical positions were different by less than three percent in the most extreme case, the variation in shutdown margin was improbable if not impossible. However, as a result of the extreme space dependence observed during the refueling (Ref 5) it was decided to perform a second shutdown margin measurement on an outer rod (#12) which was further from the detector supplying the reactivity computer. As may be seen from Table II, this additional test further demonstrated the space dependence of the MH-1A. Looking at Figure 2 one can see that as the "stuck rod" gets closer to the detector, the "shutdown margin" decreases. This is in direct contradiction to the critical bank positions.

In all cases the required shutdown margin of -1.0 percent $\Delta k/k$ (-\$1.37) was far exceeded. The shutdown margin measured for rod #5 (-\$2.60) is the least conservative value, and it is almost double the required margin. It is also, on the basis of engineering judgement, the most realistic.

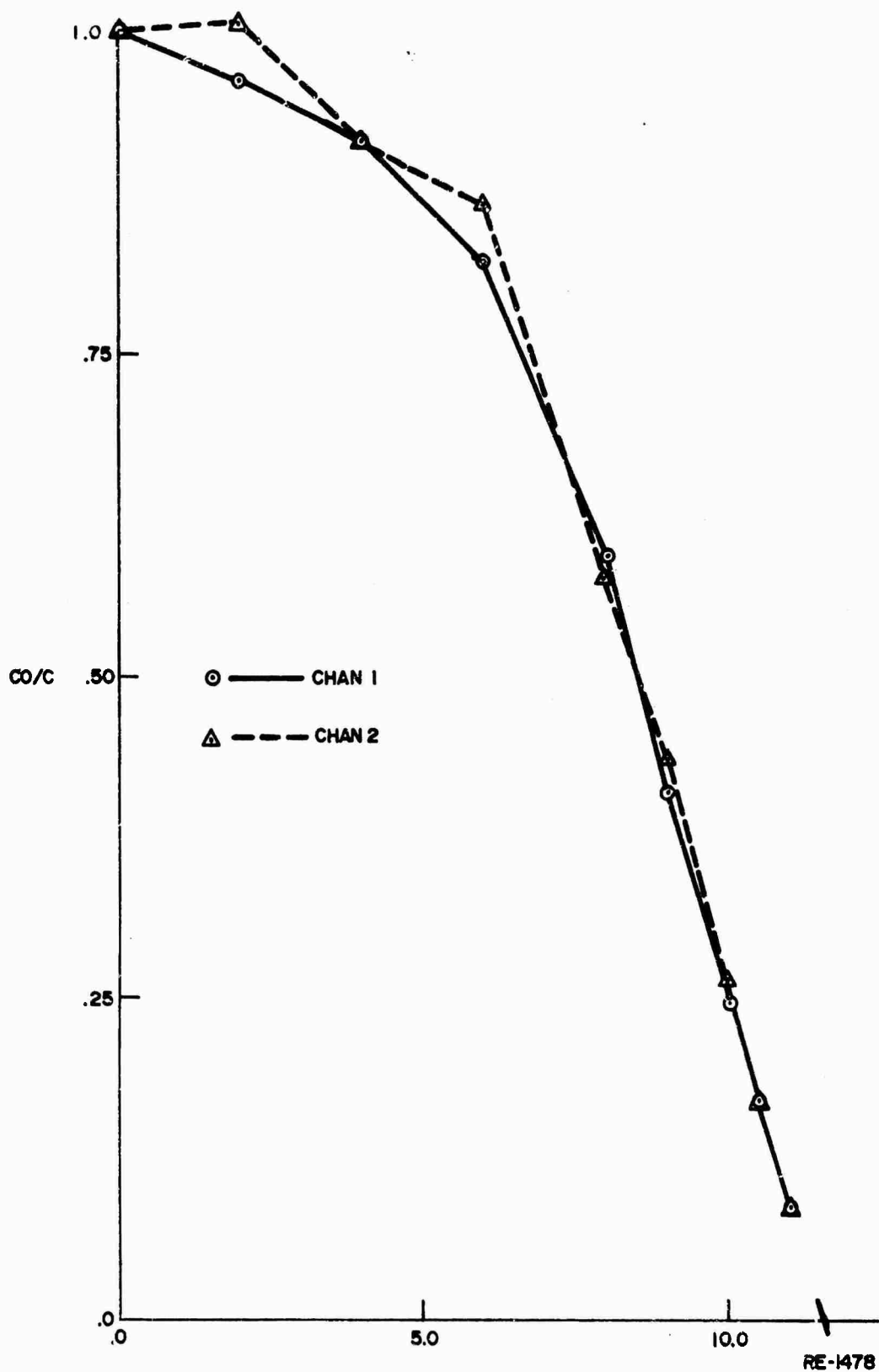


FIGURE 1. INITIAL APPROACH TO CRITICALITY

TABLE II
STUCK ROD SHUTDOWN MARGIN MEASUREMENTS

Control Rod #	Position (inches)	11 Rod Bank (inches)	Shutdown Check	Prim Temp (°F)	Prim Pres (psig)
2	35.84	9.89	- - -	152	319
1	35.73	9.89	-\$4.60	150	330
8	35.89	10.18	- - -	145	345
5	36.10	10.10	-\$2.60	147	340
12	35.96	10.00	-\$3.60	147	320

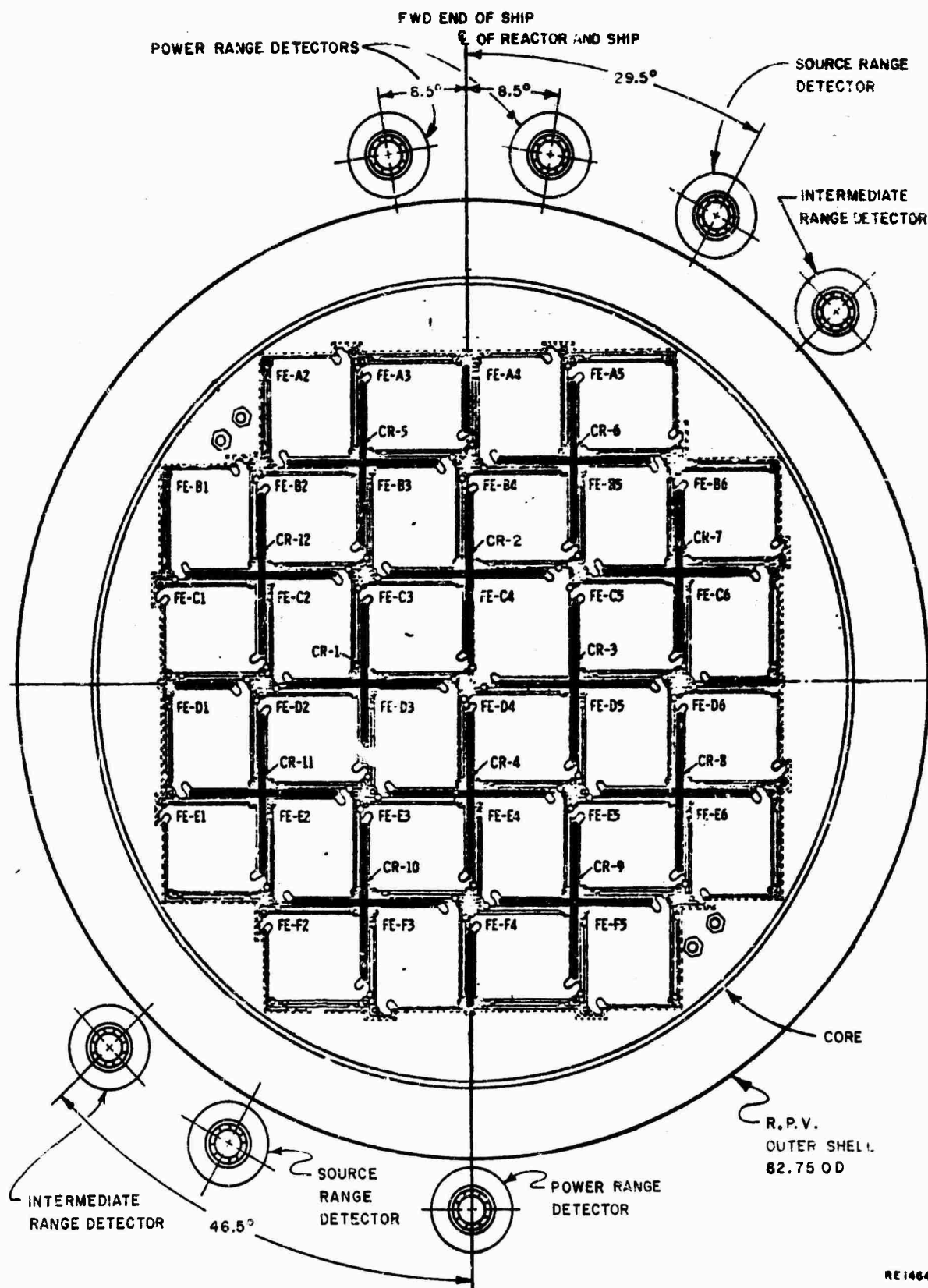


FIGURE 2. CORE - DETECTOR ORIENTATION

C. Control Rod Calibrations

The calibrations of control rods #1 and #12 were performed on 11 November 1969 and 15 November 1969; the "cold" calibrations being performed on the former date and the "hot" calibrations on the latter date. Each rod was calibrated singly against the 11-rod bank of the remaining rods. The rod being calibrated was withdrawn an amount sufficient to produce a desired positive reactivity insertion. The magnitude of the insertion was then read from the reactivity computer. After the reading was completed, the 11-rod bank was moved so as to make the reactor slightly subcritical, and the negative reactivity insertion was determined by the computer. This process was repeated until the rod being calibrated was fully withdrawn.

Table III compares the fully withdrawn integral worths for rod #1 and rod #12 for this core and its predecessor (Ref 1). Note that the information from the October 1968 report has been extrapolated slightly so that it represents the expected fully withdrawn value. It should also be noted that since rod #5 and #12 are both outer rods, it is valid for them to be compared directly.

The rod worths measured in November 1969 are vastly different from those of the October 1968 report. At first glance it would appear that it is impossible to make any comparisons. This is not the case however. The reactivity worth ratios (hot and cold) of rods #1 and #12 are directly comparable to those for rods #1 and #5. The ratios for the hot conditions differ by less than 6 percent, while those for the cold conditions differ by less than 2 percent.

This excellent agreement indicates that the method which produced the data for the October 1968 report and the November 1969 data were consistent.

Since the cores investigated for each of the tests are different, it is difficult to draw any conclusions or comparisons between actual numerical values. A general comment may be made however. The shuffled core exhibits a much smaller loss in rod worth in going from the "cold" to the "hot" condition than did the original core at BOL. The data indicates that this is a true effect and is not due to a measurement error.

Tables IV through VII summarize the measured values of reactivity (differential and integral) as a function of rod position. Figures 3 and 4 indicate the values of integral rod worth as a function of rod position.

TABLE III
FULLY WITHDRAWN INTEGRAL ROD WORTHS

	Rod #1	Rod #5	Rod #12
Nov 1969	\$2.84 (35.7 in, 484°F)	- - -	\$1.53 (36.0 in, 489°F)
(Ref 1) Oct 1968	\$1.92 (35.7 in, 479°F)	\$1.15 (36.0 in, 479°F)	- - -
Nov 1969	\$3.18 (35.7 in, 147°F)	- - -	\$2.33 (36.0 in, 147°F)
(Ref 1) Oct 1968	\$3.70 (35.7 in, 101°F)	\$2.78 (36.0 in, 101°F)	- - -

Figure 3a and 3b shows the differential rod worth increases during the last 9 inches of travel. This is explained by noting that the last 9 inches of the control rod follower have no burnable poisons, and that this section of the follower is moving into a relatively high flux peak. In figure 4a this effect occurs only to a small degree since the bank is much lower in this case. These two types of behavior were also observed in the core physics measurements of the previous core (Ref 1).

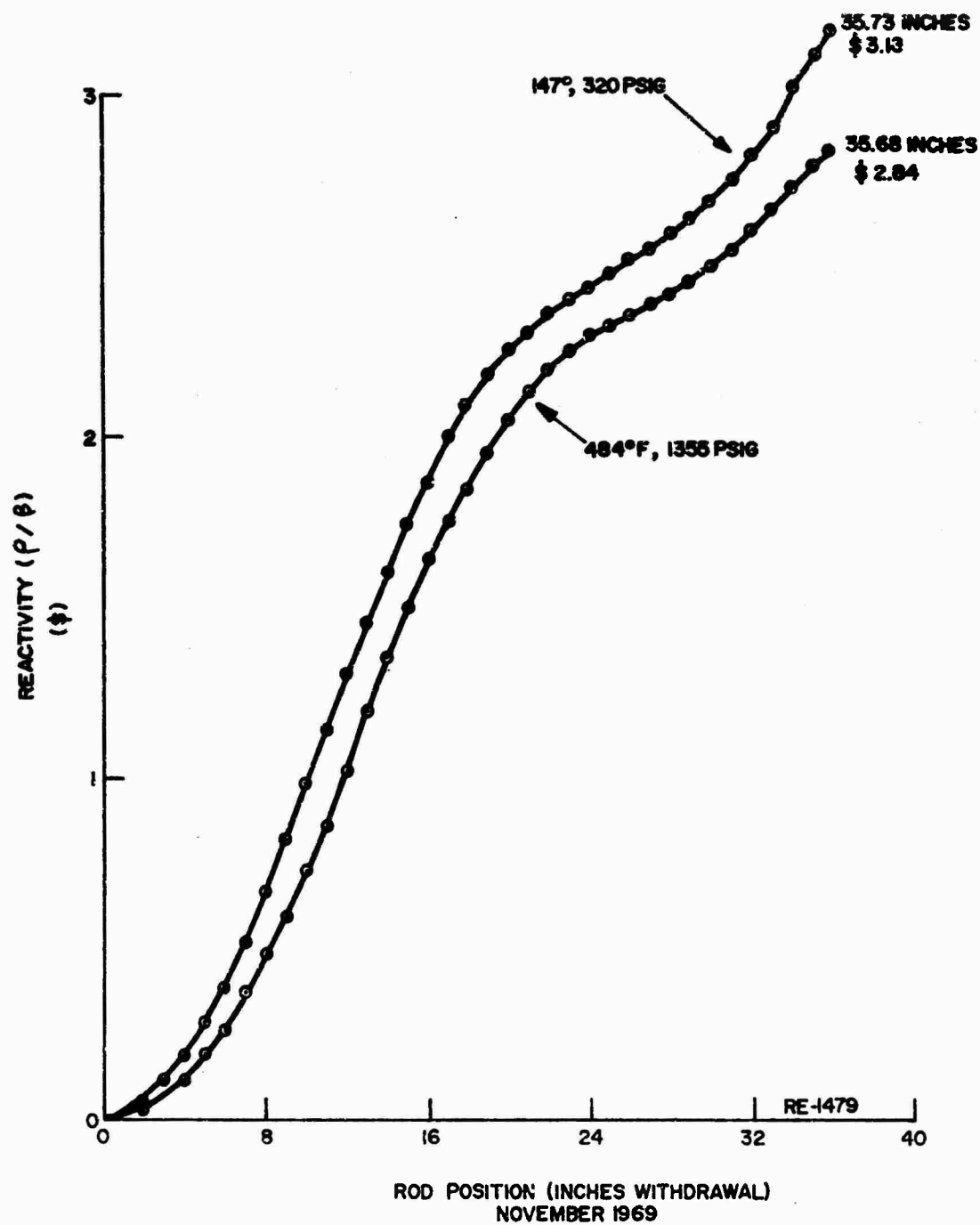


FIGURE 3. CONTROL ROD #1 INTEGRAL WORTH CURVES

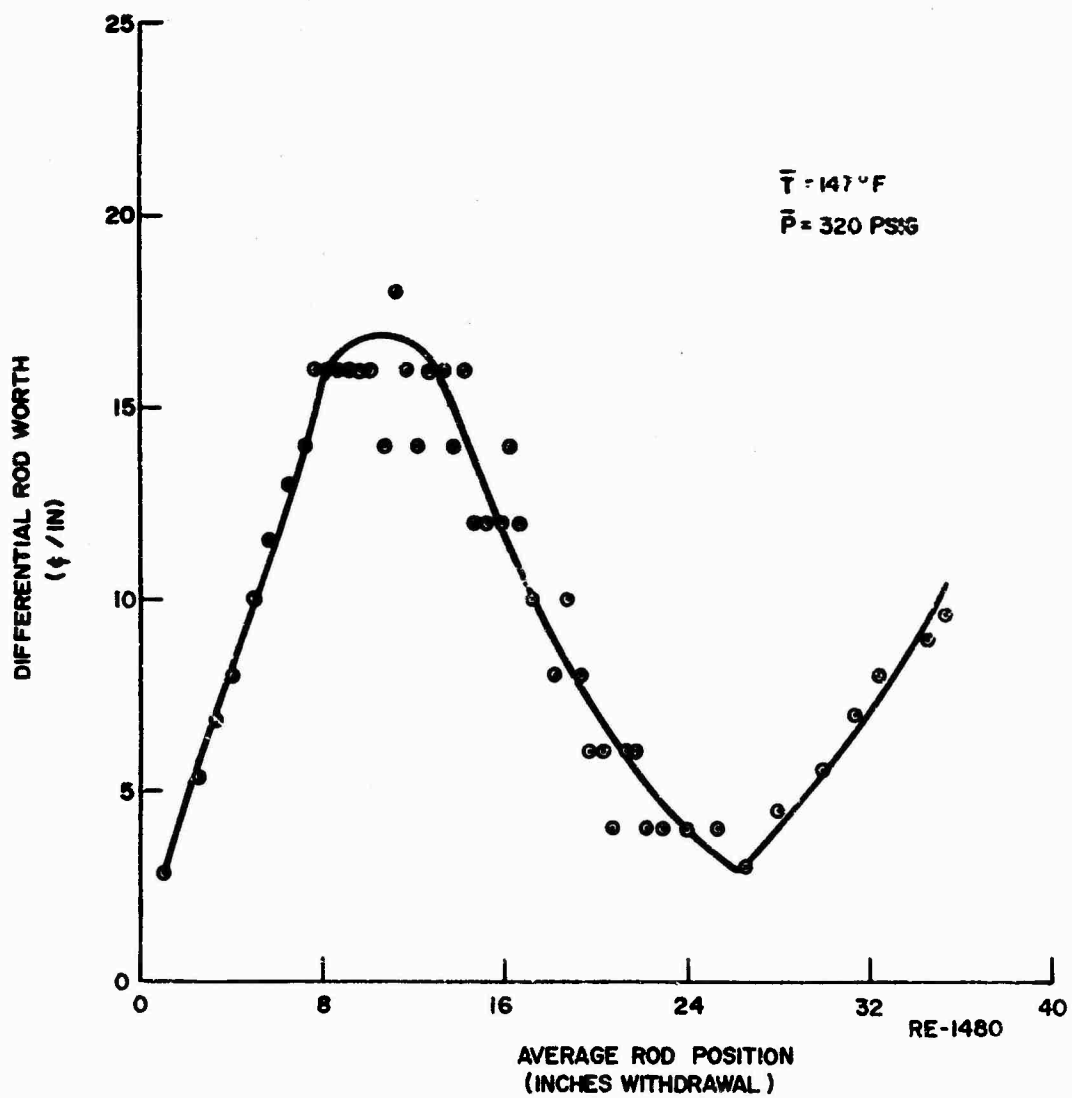


FIGURE 3a. CONTROL ROD #1 DIFFERENTIAL WORTH CURVE

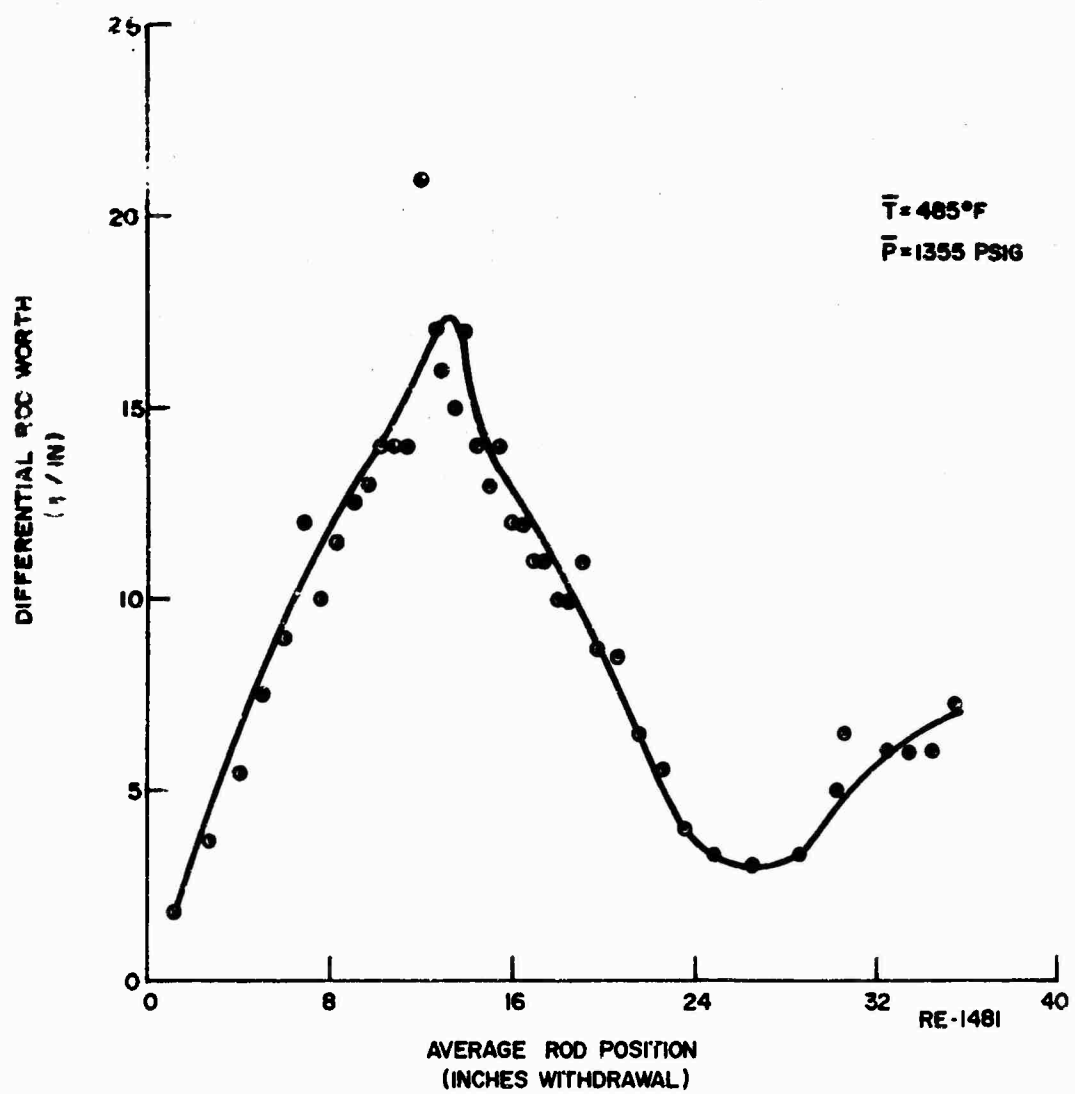


FIGURE 3b. CONTROL ROD #1 DIFFERENTIAL WORTH CURVE

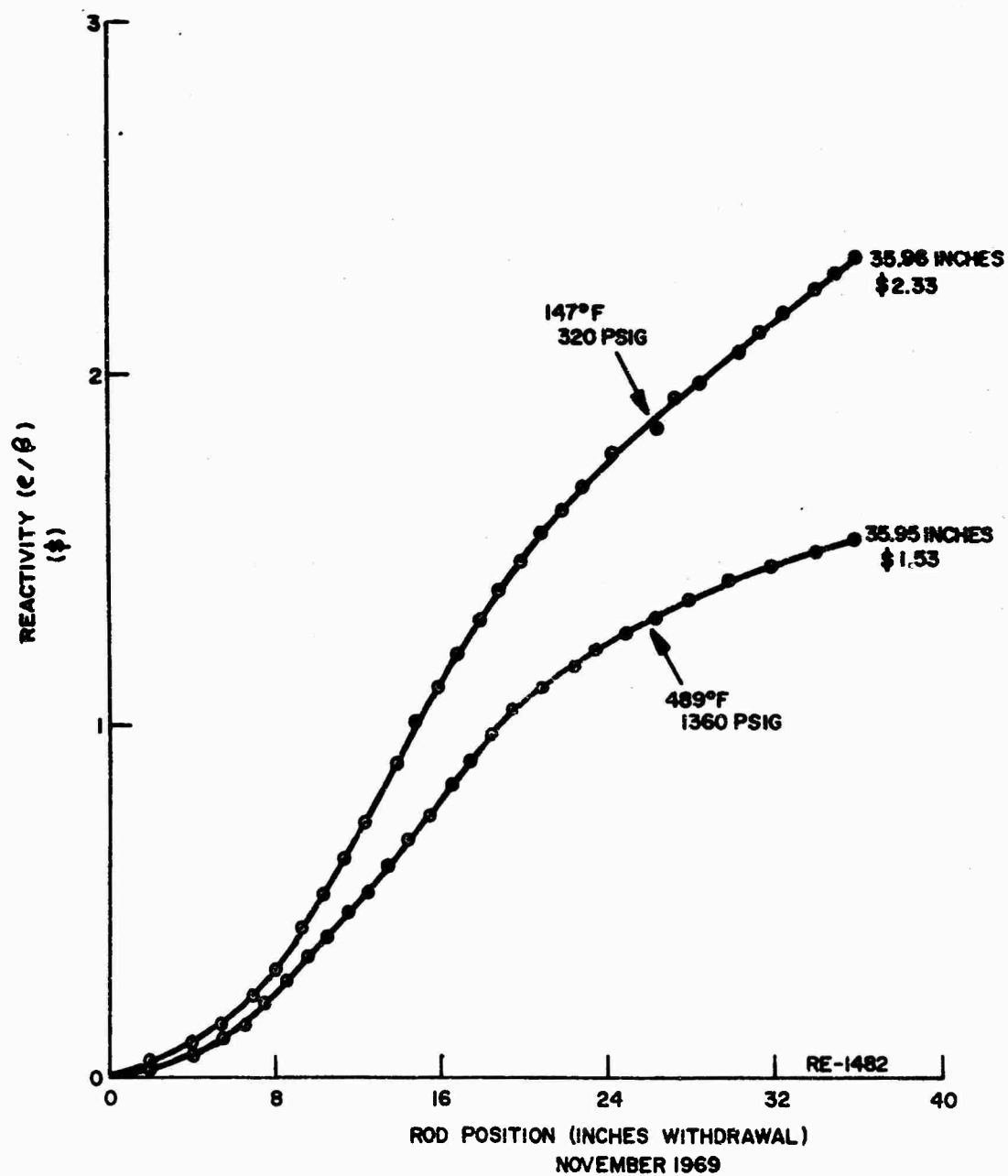


FIGURE 4. CONTROL ROD #12 INTEGRAL WORTH CURVES

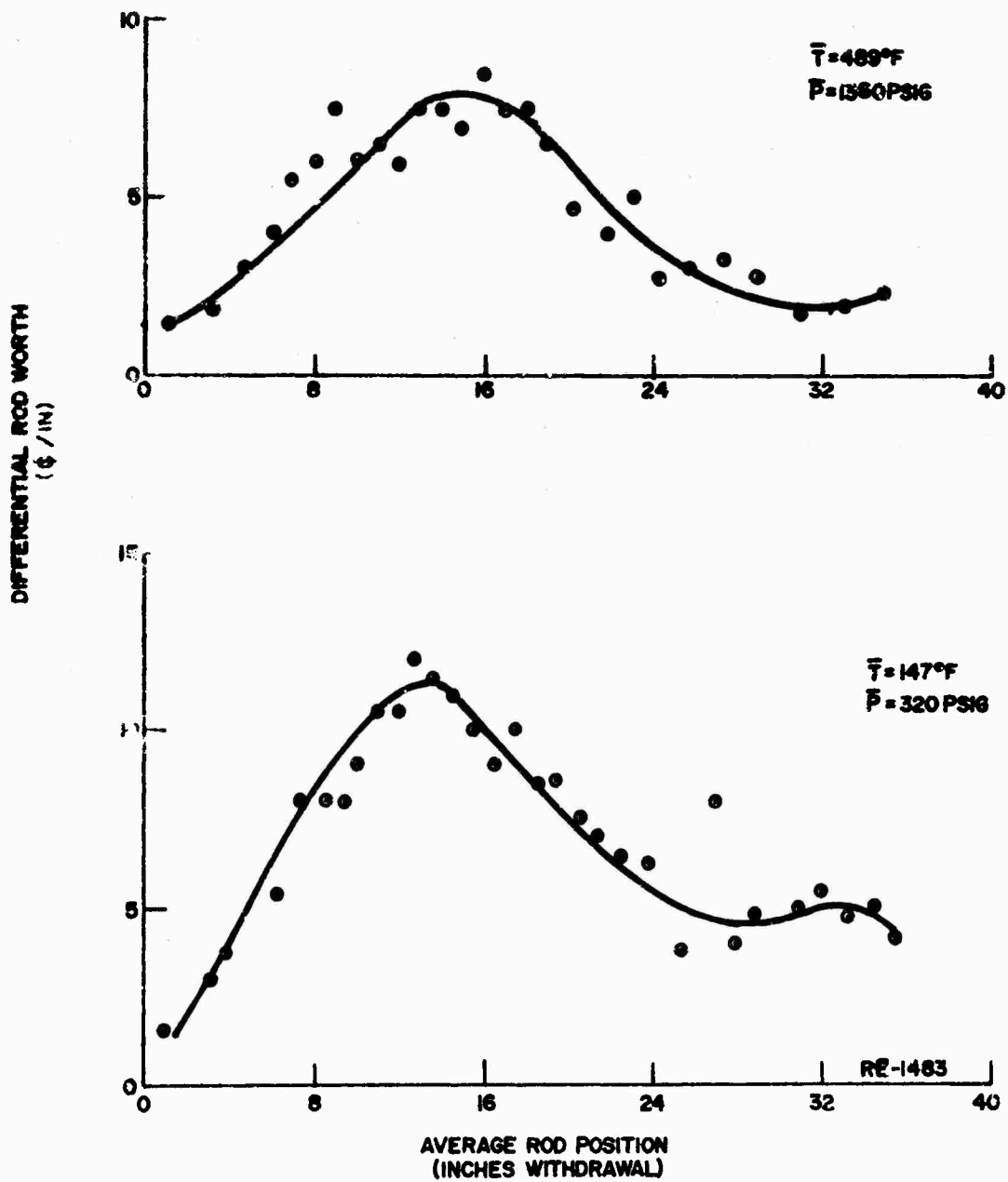


FIGURE 4a. CONTROL ROD #12 DIFFERENTIAL WORTH CURVES

TABLE IV

Control Rod #1 Calibration at 147°F, 320 psig, 11 Nov 1969

Rod Position (Inches Withdrawn)			Reactivity		
Before	After	Average	(β)	Integral (β)	c/inch
0.05	2.00	1.00	.056	.056	2.8
2.00	3.00	2.50	.054	.110	5.4
3.00	3.50	3.25	.034	.144	6.8
3.50	4.50	4.00	.08	.224	8
4.50	5.50	5.00	.10	.324	10
5.50	6.00	5.75	.058	.382	11.6
6.00	7.00	6.50	.13	.512	13
7.00	7.50	7.25	.07	.582	14
7.50	8.00	7.75	.08	.662	16
8.00	8.50	8.25	.08	.742	16
8.50	9.00	8.75	.08	.822	16
9.00	9.50	9.25	.08	.902	16
9.50	10.00	9.75	.08	.982	16
10.00	10.50	10.25	.08	1.062	16
10.50	11.00	10.75	.07	1.132	14
11.00	11.50	11.25	.09	1.222	18
11.50	12.00	11.75	.08	1.302	16
12.00	12.50	12.25	.07	1.372	14
12.50	13.00	12.75	.08	1.452	16
13.00	13.50	13.25	.08	1.532	16
13.50	14.00	13.75	.07	1.602	14
14.00	14.50	14.25	.08	1.682	16
14.50	15.00	14.75	.06	1.742	12
15.00	15.50	15.25	.06	1.802	12

Page 1 of 2

TABLE IV

Control Rod #1 Calibration at 147°F, 320 psig, 11 Nov 1969

Rod Position (Inches Withdrawn)			Reactivity		
Before	After	Average	(β)	Integral (β)	c/inch
15.50	16.00	15.75	.06	1.862	12
16.00	16.50	16.25	.07	1.932	14
16.50	17.00	16.75	.06	1.992	12
17.00	17.50	17.25	.05	2.042	10
17.50	18.00	17.75	.05	2.092	10
18.00	18.50	18.25	.04	2.132	8
18.50	19.00	18.75	.05	2.182	10
19.00	19.50	19.25	.04	2.222	8
19.50	20.00	19.75	.03	2.252	6
20.00	20.50	20.25	.03	2.282	6
20.50	21.00	20.75	.02	2.302	4
21.00	21.50	21.25	.03	2.332	6
21.50	22.00	21.75	.03	2.362	6
22.00	22.50	22.25	.02	2.382	4
22.50	23.50	23.00	.04	2.422	4
23.50	24.50	24.00	.04	2.462	4
24.50	26.00	25.25	.06	2.522	4
26.00	27.00	26.50	.03	2.552	3
27.00	29.00	28.00	.09	2.642	4.5
29.00	31.00	30.00	.11	2.752	5.5
31.00	32.00	31.50	.07	2.822	7
32.00	33.00	32.50	.08	2.902	8
33.00	34.00	33.50	.12	3.022	12
34.00	35.00	34.50	.09	3.112	9
35.00	35.73	35.36	.07	3.182	9.6

TABLE V

Control Rod #1 Calibration at 485°F, 1355 psig, 15 Nov 1969

Rod Position (Inches Withdrawn)			Reactivity		
Before	After	Average	(β)	Integral (β)	β /inch
0.059	2.00	1.03	.035	.035	.018
2.0	3.5	2.75	.055	.090	.037
3.5	4.5	4.0	.055	.145	.055
4.5	5.5	5.0	.075	.220	.075
5.5	6.5	6.0	.090	.310	.090
6.5	7.25	6.88	.09	.400	.120
7.25	8.00	7.63	.075	.475	.100
8.00	8.75	8.38	.085	.560	.114
8.75	9.50	9.13	.095	.655	.126
9.50	10.00	9.75	.065	.720	.130
10.00	10.5	10.25	.07	.790	.140
10.5	11.25	10.88	.105	.895	.140
11.25	11.75	11.50	.07	.965	.140
11.75	12.25	12.00	.105	1.070	.210
12.25	12.75	12.50	.085	1.155	.170
12.75	13.25	13.00	.08	1.235	.160
13.25	13.75	13.50	.075	1.310	.150
13.75	14.25	14.00	.085	1.395	.170
14.25	14.75	14.50	.07	1.465	.140
14.75	15.25	15.00	.065	1.530	.130
15.25	15.75	15.50	.070	1.600	.140
15.75	16.25	16.00	.06	1.660	.120

TABLE V

Control Rod #1 Calibration at 485°F, 1355 PSIG, 15 Nov. 1969

Rod Position (Inches Withdrawn)			Reactivity		
Before	After	Average	(β)	Integral (β)	β /inch
16.25	16.75	16.50	.060	1.720	.120
16.75	17.25	17.00	.055	1.775	.110
17.25	17.75	17.50	.055	1.830	.110
17.75	18.25	18.00	.050	1.880	.100
18.25	18.75	18.50	.05	1.930	.100
18.75	19.25	19.00	.055	1.985	.110
19.25	20.00	19.63	.065	2.050	.087
20.00	21.00	20.50	.085	2.135	.085
21.00	22.00	21.50	.065	2.200	.065
22.00	23.00	22.50	.055	2.255	.055
23.00	24.00	23.50	.04	2.295	.040
24.00	25.50	24.75	.050	2.345	.033
25.50	27.50	26.50	.060	2.405	.030
27.50	29.50	28.50	.065	2.470	.0325
29.50	31.00	30.25	.075	2.545	.050
31.00	32.00	31.50	.065	2.610	.065
32.00	33.00	32.50	.060	2.670	.060
33.00	34.00	33.50	.06	2.730	.060
34.00	35.00	34.50	.06	2.790	.060
35.00	35.68	35.34	.05	2.840	.073

TABLE VI

Control Rod #12 Calibration at 147°F, 320 PSIG, 11 Nov. 1969

Rod Position (Inches Withdrawn)			Reactivity		
Before	After	Average	(ρ)	Integral (ρ)	ρ /inch
0.00	2.00	1.00	.030	.030	.015
2.00	4.00	3.00	.060	.090	.030
4.00	5.50	4.75	.055	.145	.037
5.50	7.00	6.25	.080	.225	.053
7.00	8.00	7.50	.080	.305	.080
8.00	9.00	8.50	.080	.385	.080
9.00	9.50	9.25	.040	.425	.080
9.50	10.50	10.00	.090	.515	.090
10.50	11.50	11.00	.105	.620	.105
11.50	12.5	12.0	.105	.725	.105
12.5	13.0	12.75	.060	.785	.120
13.0	14.0	13.5	.115	.900	.115
14.0	15.0	14.5	.110	1.010	.110
15.0	16.0	15.5	.100	1.110	.100
16.0	17.0	16.5	.090	1.200	.090
17.0	18.0	17.5	.100	1.300	.100
18.0	19.0	18.5	.085	1.385	.085
19.0	20.0	19.5	.085	1.470	.085
20.0	21.0	20.5	.075	1.545	.075
21.0	22.0	21.5	.070	1.615	.070
22.0	23.0	22.5	.065	1.680	.065
23.0	24.5	23.75	.095	1.775	.063

Control Rod #12 Calibration at 147°F, 320 PSIG, 11 Nov. 1969

Page 2 of 2

TABLE VII
Control Rod #12 Calibration at 489°F, 1360 PSIG, 15 Nov. 1969

Rod Position (Inches Withdrawn)			Reactivity		
Before	After	Average	(β)	Integral (β)	β /Inch
0.20	2.00	1.10	.025	.025	.014
2.00	4.00	3.00	.035	.060	.018
4.00	5.50	4.75	.045	.105	.030
5.50	6.50	6.00	.040	.145	.040
6.50	7.50	7.00	.055	.200	.055
7.50	8.50	8.00	.060	.260	.060
8.50	9.50	9.00	.075	.335	.075
9.50	10.51	10.00	.060	.395	.060
10.51	11.50	11.00	.065	.460	.065
11.50	12.5	12.0	.060	.520	.060
12.5	13.50	13.0	.075	.595	.075
13.50	14.50	14.00	.075	.670	.075
14.50	15.50	15.00	.070	.740	.070
15.50	16.50	16.00	.085	.825	.085
16.50	17.50	17.00	.075	.900	.075
17.50	18.50	18.00	.075	.975	.075
18.50	19.50	19.00	.065	1.040	.065
19.50	21.00	20.25	.070	1.110	.047
21.00	22.50	21.75	.060	1.170	.040
22.50	23.50	23.00	.050	1.220	.050
23.50	25.00	24.25	.040	1.260	.027

Control Rod #12 Calibration at 489°F, 1360 PSIG, 15 Nov. 1969

Page 2 of 2

D. Temperature Coefficient of Reactivity

The temperature coefficient measurement was performed on 11 November 1969 (lower temperature range) and 15 November 1969 (upper temperature range). The temperature coefficient was measured by establishing a primary system linear heat-up rate of $\sim 60^\circ\text{F}$ per hour and recording the changes in temperature and reactivity as a function of time during the heat-up. The heat-up was accomplished by using both pump heat and reactor heat. From this data, an expression for both the reactivity and the temperature as a quadratic function of time was found, fitting the data by the method of moments. The resulting expressions were:

$$\left. \begin{aligned} R(t) &= 4.0 \times 10^{-5} t^2 + 1.05 \times 10^{-2} t - 3.5 \times 10^{-2} \\ T(t) &= 1.9 \times 10^{-4} t^2 + 7.29 \times 10^{-1} t + 1.83 \times 10^2 \end{aligned} \right\} \quad \text{11 Nov data}$$

$$\left. \begin{aligned} R(t) &= 2.0 \times 10^{-5} t^2 + 1.95 \times 10^{-2} t - 4.3 \times 10^{-3} \\ T(t) &= -3.7 \times 10^{-4} t^2 + 1.066 t + 2.42 \times 10^2 \end{aligned} \right\} \quad \text{15 Nov data}$$

where time t is in minutes, reactivity R is in β , and temperature T is in $^\circ\text{F}$.

From these fitted curves, the temperature coefficient is calculated thus:

$$\frac{\Delta R}{\Delta T} (\bar{T}) = \frac{R(t+t') - R(t)}{T(t+t') - T(t)}$$

where t' is the increment between successive time steps ($t' = 10$ minutes was used) and \bar{T} is the average temperature over the time step, $\bar{T} = T(t+5t')$.

Figure 5 illustrates the results. Note that the data on the two days demonstrates contradictory trends: The data of 11 November results in a curve whose slope decreases as temperature increases, while the data of 15 November shows an opposite trend. The curve of 11 November is in error due to variations in heat-up rate, filling of the steam generator, and lack of overall experience in running the temperature coefficient measurements with the reactivity computer. The data of 15 November shows much better results. All the data was used however, in order to provide information over the entire operating range of the reactor.

Using the data of Figure 5, a single quadratic curve was found, again by the method of moments, to give the best fit to the data:

$$\frac{\Delta \rho}{\Delta T} = 4.39 \times 10^{-8} T^2 + 2.84 \times 10^{-5} T + 9.0 \times 10^{-3} \quad (\beta/^\circ\text{F})$$

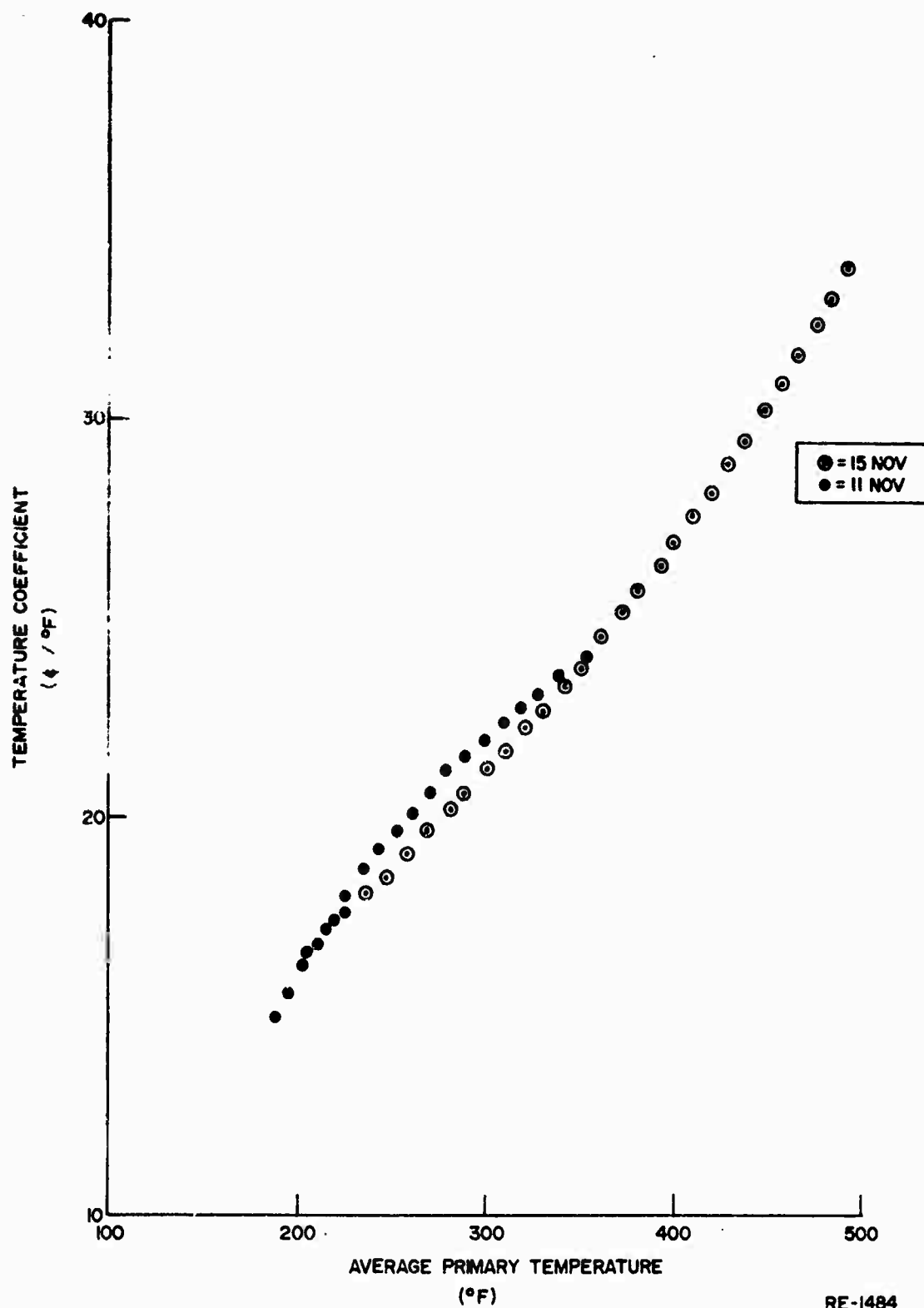


FIGURE 5. TEMPERATURE COEFFICIENT DATA

This curve is plotted in Figure 6. At 68°F, it yields a temperature coefficient of reactivity of $-1.11\text{c}/^\circ\text{F}$ or $-8.10 \times 10^{-5}/^\circ\text{F}$. At 490°F, it yields a temperature coefficient of $-3.35\text{c}/^\circ\text{F}$ or $-2.45 \times 10^{-4}/^\circ\text{F}$. The temperature defect is found by integration of the quadratic expression:

$$\Delta \rho (\Delta T) = \int_{68}^{490} \frac{\Delta \rho}{\Delta T} dt = \$8.86 \text{ or } 6.47\% \Delta \rho$$

Table VIII compares these results with previous values.

The accuracy of fit of the quadratic expression to the data may be measured by adding up the reactivity change contributions (see Tables IX and X) over the entire temperature range, and comparing this to the \$8.86 obtained above. Since the data only begins at 185°F, the contribution from 68°F to 185°F was assumed to be well represented by the integration of the quadratic expression:

$$\int_{68}^{185} \left(\frac{\Delta \rho}{\Delta T} \right) dT = \$1.56$$

From 185°F to 490°F, the $\Delta \rho$ values were added up (see Tables IX and X), yielding \$7.41. Thence the temperature defect was found by adding up the raw data result and the correction back to 68°F.

$$\Delta \rho (\Delta T) = \$7.41 + \$1.56 = \$8.97$$

This result agrees to within 1.2 percent of the result obtained by integrating the quadratic fit (which smooths out fluctuations in the data); thus, the quadratic curve represents well the true temperature coefficient behavior in a smoothed-out sense.

TABLE VIII

TEMPERATURE COEFFICIENT			
Temperature	Experimental		Theoretical (Ref 2)
	Nov 69	Oct 68 (Ref 1)	
68°F	-8.10×10^{-5}	-3.0×10^{-5}	$-3.3 \times 10^{-5}/^\circ\text{F}$
490°F	-2.45×10^{-4}	-2.95×10^{-4}	$-2.7 \times 10^{-4}/^\circ\text{F}$
TEMPERATURE DEFECT			
	6.47% $\Delta \rho$	6.4% $\Delta \rho$	4.8% $\Delta \rho$

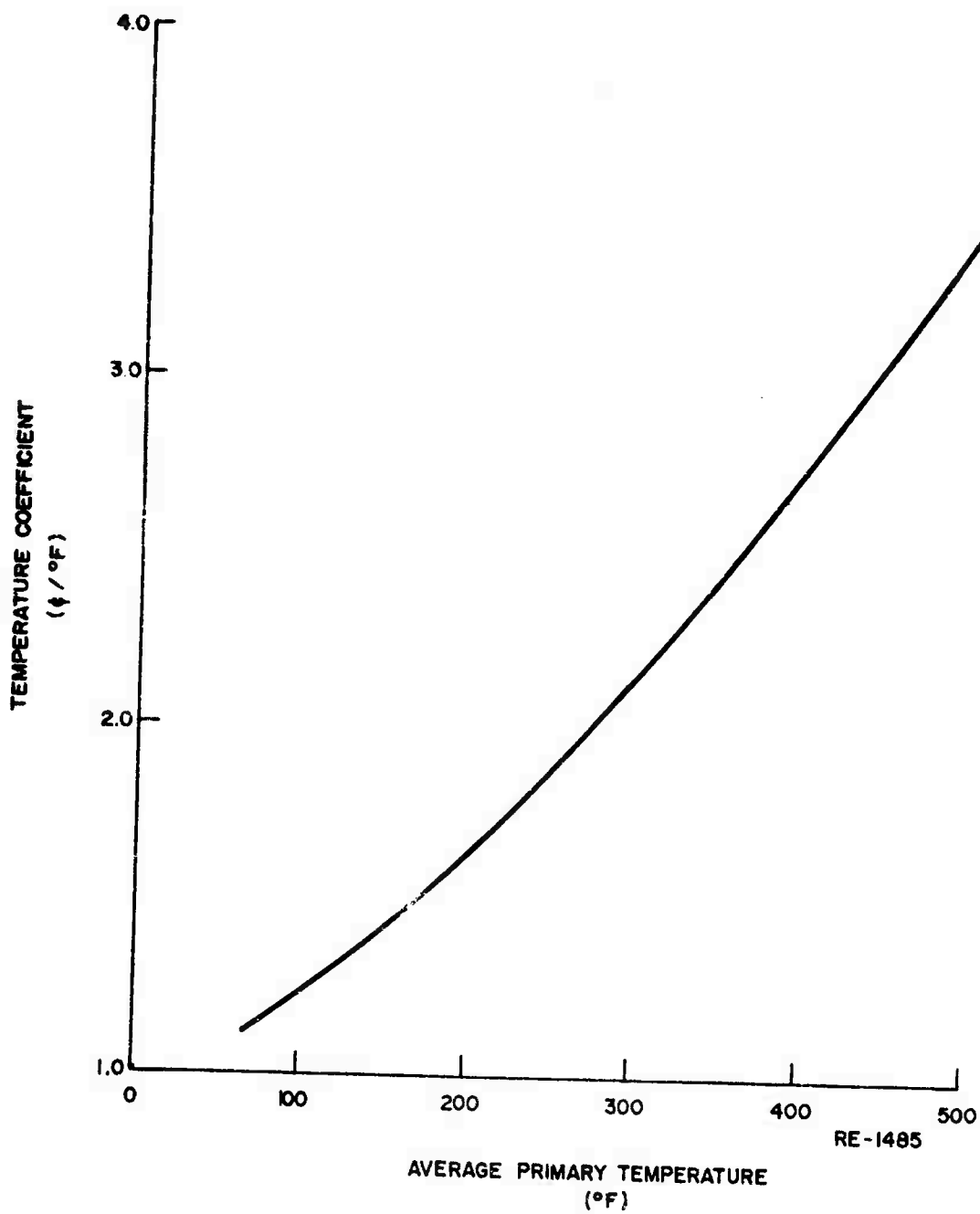


FIGURE 6. QUADRATIC CURVE FIT TO TEMPERATURE COEFFICIENT DATA

The data yields a $\Delta\rho/\Delta T$ much larger at low temperature than the theoretical value. However, better agreement (about 16 percent low) is obtained at the upper temperature. Though the value of the temperature defect differs significantly from the theoretical value (4.8 percent $\Delta\rho$), it agrees well with the value measured for the previous core (6.8 percent $\Delta\rho$). Hence, the $\Delta\rho/\Delta T$ versus T behavior of the two cores is nearly the same in an integral sense, even though there appears to be a variance in low temperature behavior.

TABLE IX
Temperature Coefficient

Date: 11 Nov 1969

Stopwatch Time (Min)	Average Primary Temperature (°F)	Primary Pressure (psig)	Average 12 Rod Bank Position (Inches)	Reactivity Change (\$)
0	185	330	11.92	0
3	188	330	11.95	.04
8	191	330	11.98	.04
14	194	330	12.03	.07
19	197	330	12.07	.055
25	202	335	12.12	.055
30	204	335	12.16	.035
37	211	335	12.24	.105
45	217	335	12.30	.06
50	220	335	12.36	.08
56	225	335	12.42	.08
61	230	335	12.49	.08
65.5	234	338	12.55	.11
69	237	340	12.60	.065
75	245	335	12.70	.125
78-80	246	340	12.70	-.01
83	248	340	12.78	.08
87	253	340	12.84	.095

**

** Steam Generator Filling

TABLE IX (CONT'D)
Temperature Coefficient

Date: 11 Nov 1969

[illegible]

TABLE X
Temperature Coefficient

Date: 15 Nov 1969

Stopwatch Time (Min)	Average Primary Temperature (°F)	Primary Pressure (psig)	Average 12 Rod Bank Position inches	Reactivity Change (\$)
0	247	340	12.47	0
7	252	340	12.54	.10
13	257	350	12.62	.085
22	264	380	12.74	.175
27	267	400	12.84	.105
32	275	400	12.92	.115
39	282	400	13.04	.13
45	287	400	13.15	.11
49	290	410	13.21	.10
54	294	435	13.30	.115
59	301	460	13.40	.095
64	307	480	13.51	.135
71	315	519	13.64	.145
76	320	549	13.77	.15
82	328	575	13.94	.165
88	336	575	14.08	.18
94	341	590	14.20	.115
100	347	630	14.32	.135
105	351	660	14.41	.105
111	358	700	14.56	.145
116	363	730	14.66	.12
120	366	760	14.78	.12
125	371	800	14.88	.095

TABLE X
Temperature Coefficient

Stopwatch Time (Min)	Average Primary Temperature (°F)	Primary Pressure (psig)	Average 12 Rod Bank Position (inches)	Reactivity Change (\$)
130	376	830	15.00	.125
135	381	870	15.13	.115
140	385	900	15.24	.115
146	390	950	15.40	.155
152	397	990	15.53	.13
157	401	1030	15.65	.11
162	405	1080	15.77	.115
166	409	1110	15.86	.085
171	413	1160	15.99	.105
175	417	1200	16.11	.16
180	421	1240	16.19	.03
185	425	1290	16.33	.12
190	429	1335	16.47	.13
196	435	1380	16.63	.15
200	439	1375	16.76	.115
203	442	1385	16.87	.085
208	447	1385	17.03	.14
212	451	1382	17.20	.13
216	454	1365	17.35	.125
220	458	1355	17.52	.125
224	462	1365	17.63	.10
227	464	1363	17.78	.13
230	468	1360	17.94	.12
237	475	1360	18.23	.20

TABLE X
Temperature Coefficient

Stopwatch Time (Min)	Average Primary Temperature (°F)	Primary Pressure (psig)	Average 12 Rod Bank Position (inches)	Reactivity Change (\$)
241	478	1370	18.40	.13
245	482	1358	18.61	.15
248	485	1350	18.78	.14
254	491	1372	19.03	.165

E. Power Coefficient of Reactivity

The power coefficient measurements were performed on 19 November 1969 (Section I data, increments increasing power at minimum xenon conditions) and on 25 November 1969 (Section II data, increments decreasing power from equilibrium xenon conditions). The technique employed was to increase (decrease) the reactor power by increasing (decreasing) the generator load and then recording the resulting temperature change. Knowing the temperature coefficient of reactivity, it is possible to ascertain the reactivity change caused by the change in power. Thus, the power coefficient is simply the ratio of the reactivity change to the power change, assigned to the average power in the interval of power change. Table XI shows representative recorded information for these measurements.

The resulting values of the power coefficient are presented in Figure 7. Considerable scatter is evident in the calculated values, particularly those due to the Section I data. This is due to the build-up of xenon during the measurements, resulting when a large amount of time (4-1/2 hours) was spent in making the power changes. Thus, the requirement of minimum xenon was not met for the later data of Section I, and these points (power > 30 MW) are obviously in error and were not used in computing the power coefficient. The remaining data from both Sections I and II was used in obtaining a linear curve fit, by the method of moments, shown in Figure 7. Thence the average value of the power coefficient of reactivity was found to be -4.03¢/MWT or $-2.95 \times 10^{-4}/\text{MWT}$. This is to be compared to the theoretical value of $-2.1 \times 10^{-4}/\text{MWT}$. (Ref 2). In spite of the data scatter, all the experimental values are significantly higher than the theoretical ones.

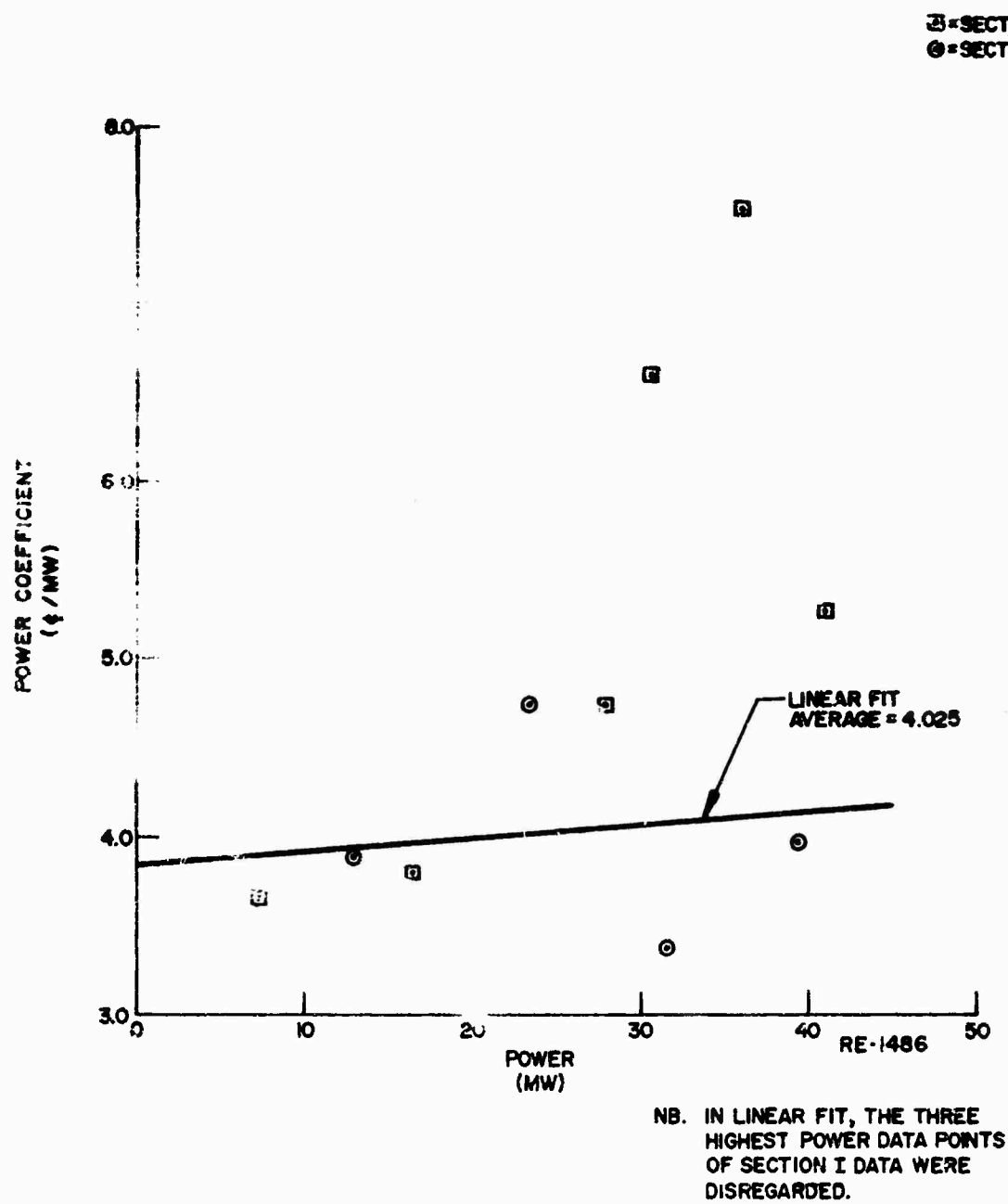


FIGURE 7. POWER COEFFICIENT DATA

The measurements of power coefficient gave poor results. The analysis of the power coefficient data was rendered difficult and some somewhat arbitrary by three lapses in experimental technique:

1. The measurements were not performed quickly enough, thus permitting xenon to build-up and obscure the data.

2. On the data recording sheets, the readings from the Keithley pico-ammeter were either omitted or illegible, making it difficult to verify the power changes or to normalize the readings of the power channels.

3. A recalibration was performed in the middle of the measurements.

TABLE XI
POWER COEFFICIENT DATA

Time (Hours)	Primary Pressure (psig)	Average Rod Bank Position (Inches)	Average Primary Temp (°F)	Power Level *(%)	Remarks
1300	1375	20.60	518	13	Start of Section I Data (19 Nov 69)
1330	1367	20.60	515	19.5	
1400	1368	20.60	498	54	
1430	1345	20.60	488	71	
1555	-	-	-	71	Recalibration of Power Level
1555	1350	21.55	514	61	
1610	1345	21.55	502	75	
1633	1365	21.55	492	85	
1656	1315	21.55	493	83.5	Start of Section II Data (25 Nov 69)
1728	1370	21.55	483	98	
1334	1365	26.70	490	95	
1338	1360	26.70	498	80	
1350	1362	26.07	490	80	
1358	1363	26.07	499	60	

* Channel 7 Data used, considered the most consistent.

TABLE XI (CONT'D)
Power Coefficient Data

Time (Hours)	Primary Pressure (psig)	Average Rod Bank Position (Inches)	Average Primary Temp (°F)	Power Level *(%)	Remarks
1413	1377	25.45	490	61	
1421	1360	25.45	502	42	
1435	1374	24.75	490	42	
1445	1370	24.75	504	15	

* Channel 7 data used, considered the most consistent.

F. Equilibrium Xenon

The xenon equilibrium measurements, with the reactor at near-full power, were performed on 19 November 1969 through 20 November 1969. The technique employed for these measurements used the previously measured temperature coefficient to ascertain the amount of poisoning caused by xenon build-up. As xenon built-up, the loss of reactivity caused by the increased absorption of neutrons was balanced by the decrease in temperature and power. Periodically the control rods were withdrawn to return the mean primary temperature to ~490°F and subsequently raise the power level. By summing the changes in primary temperature, multiplying this sum by the temperature coefficient, and adding contributions due to power changes, the negative reactivity attributable to xenon build-up was calculated.

Due to an omission in recording data, the rod bank was moved (at time = 18.13 hours) without recording the temperature; thus, this datum point could not be calculated. Instead, a method of moments linear fit (on semi-logarithmic paper, since the expected exponential form would yield a straight line) was used to predict this datum (see Figure 8). Succeeding points depended on this datum since the xenon build-up was calculated in an integral manner.

In addition to the error associated with the omitted data, is the error in overall loss of reactivity due to xenon build-up caused by the amount of time consumed in performing the power coefficient test. Since the power coefficient data is so scattered, the total amount of reactivity loss due to xenon build-up during the power coefficient measurement is hard to estimate. In addition, the time of equivalent full-power operation is also hard to estimate. From the data of Table XI, the estimated time of full-power operation can be calculated by summing

MD=MISSING DATUM
 ▲ VALUES PREDICTED FROM GRAPH
 GIVEN VALUE FOR T=18.13

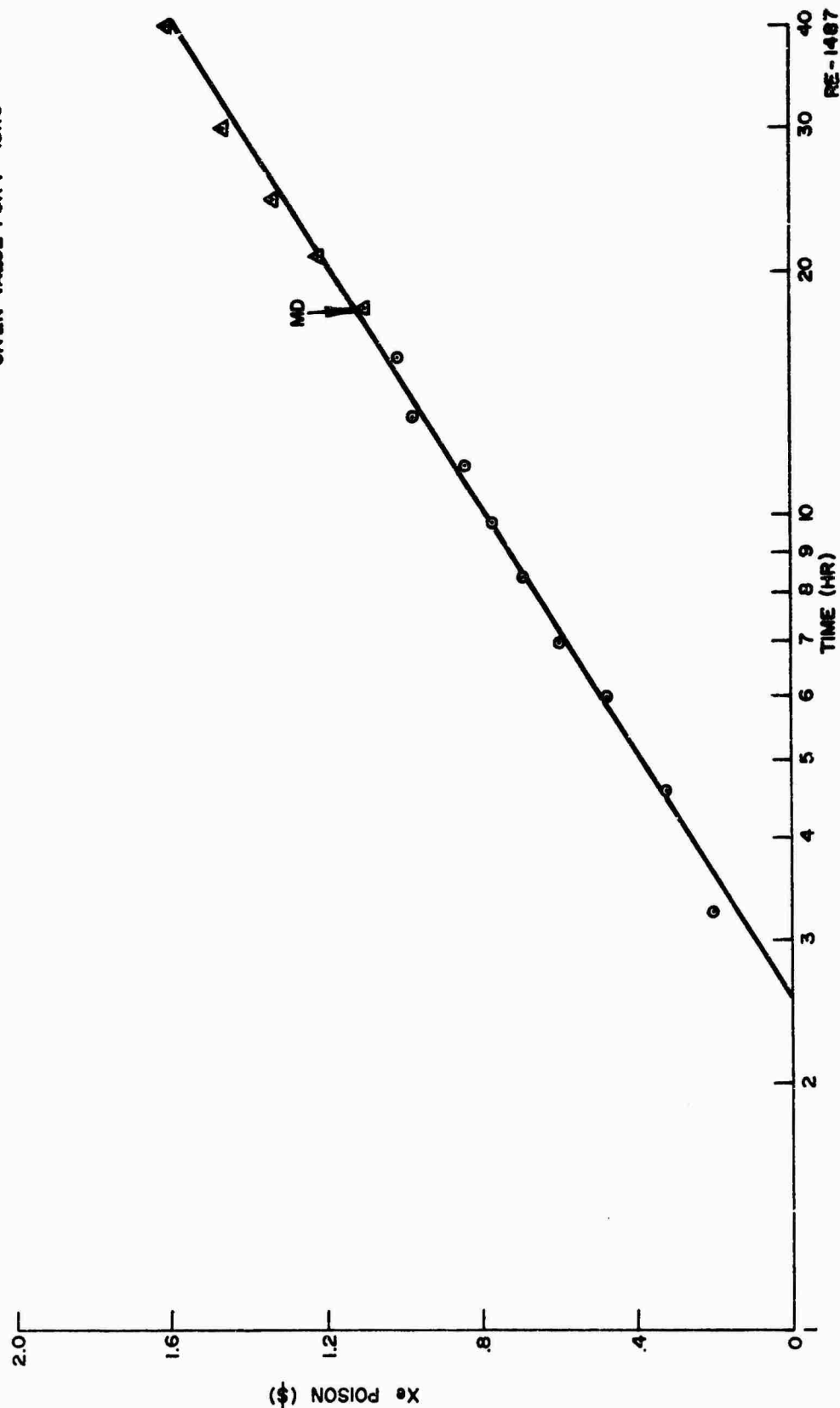
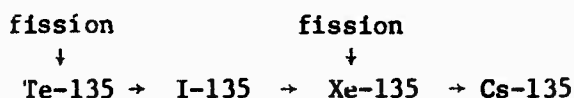


FIGURE 8. EXTRAPOLATION TO OBTAIN MISSING DATUM

the fractional power operation during each time interval. This yields 2.95 hours of equivalent full-power operation during the power coefficient measurements, equivalent to building in approximately 22¢ of xenon. Figure 9 shows the resulting time shifted data. For purposes of comparison, the theoretical curve is also presented (see below for how it was obtained). It is apparent that the data values are significantly smaller than the theoretical values. The equilibrium value obtained from the data is -1.85 or -1.4 percent $\Delta\rho$ (obtained by adding 22¢ to the asymptotic value indicated by the data in Figure 9).

It is meaningful to calculate what the number density of Xe-135 as a function of time would be from theoretical considerations, and compare it to the behavior observed in the data. Now, Xe-135 is formed by the following decay chain:



Because Te-135 decays very rapidly, the usual approximation (3) is made that I-135 is directly produced in fission.

The theoretical xenon build-up curve may be obtained by solving the following differential equations: (Ref 3),

$$\frac{dI}{dt} = AI + B$$

$$\frac{dX}{dt} = CX + \lambda_I I + D$$

where

$$A = -\lambda_I$$

$$B = \gamma_I \Sigma_f \phi$$

$$C = -(\lambda_x + \sigma_{ax} \phi)$$

$$D = \gamma_x \Sigma_f \phi$$

I = I-135 number density

X = Xe-135 number density

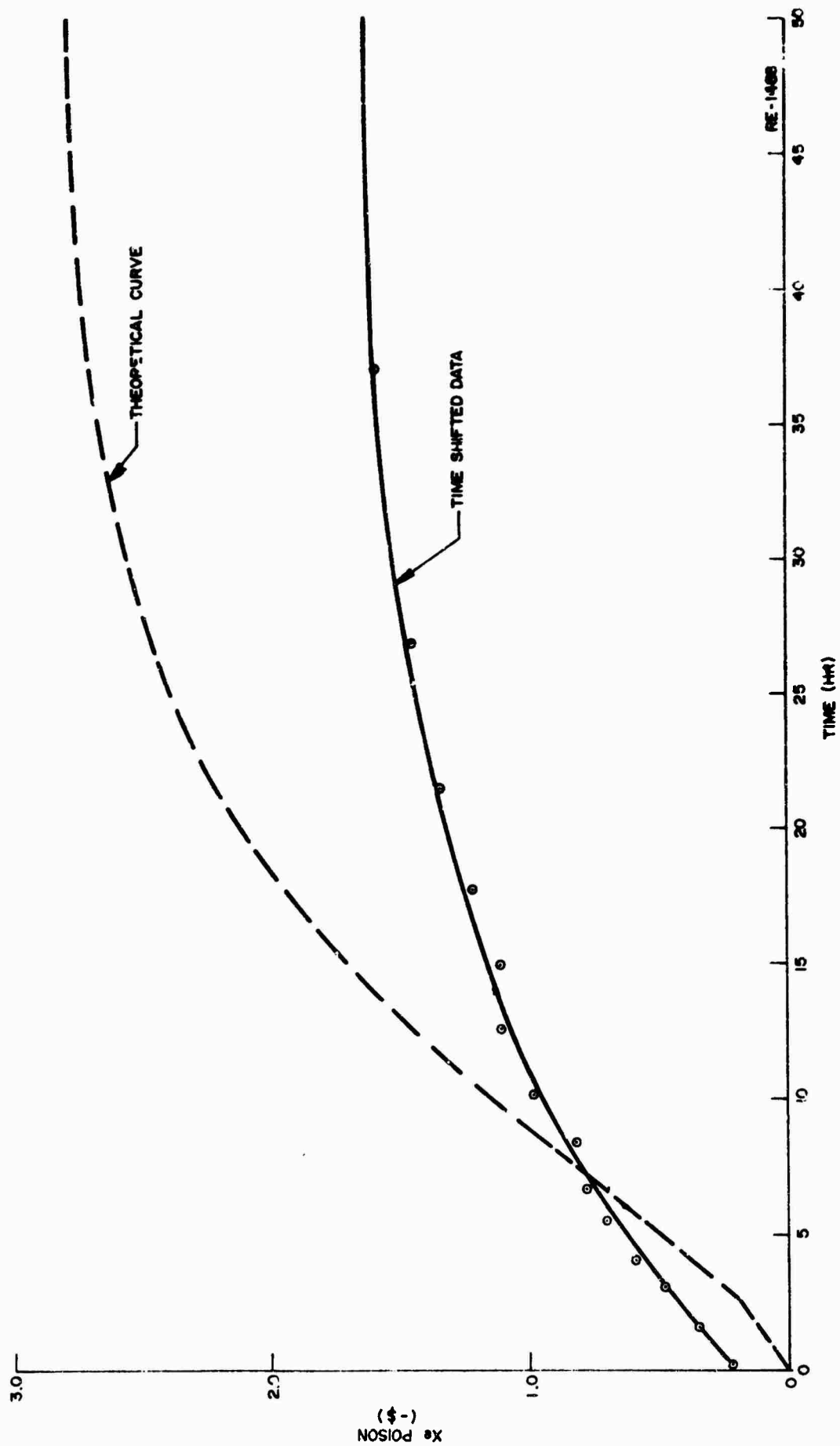


FIGURE 9. XENON BUILD-UP (EXPERIMENTAL DATA)

The resulting expression for the time-dependent xenon number density is:

$$X(t) = \frac{\gamma_X \Sigma f \phi}{\lambda_X + \sigma_{ax}} [1 - e^{-(\lambda_X + \sigma_{ax})t}] + \frac{\gamma_I \Sigma f \phi}{\lambda_X + \sigma_{ax}} \left[\frac{1}{\lambda_I + \sigma_{ax}} \left(e^{-(\lambda_X + \sigma_{ax})t} - e^{-\lambda_I t} \right) + \frac{\gamma_I \Sigma f \phi}{\lambda_X + \sigma_{ax}} \right]$$

The following parameters were used (Reference 3):

$$\sigma_{ax} = 2.7 \times 10^{-18} \text{ cm}^2$$

$$\gamma_I = 0.061$$

$$\gamma_X = 0.003$$

$$\lambda_I = 0.1035 \text{ hr}^{-1}$$

$$\lambda_X = 0.0753 \text{ hr}^{-1}$$

And the fission cross-section and number density for uranium and the thermal flux were obtained from the LEOPARD program (Ref 4):

$$\Sigma_{f235} = N_{235} \sigma_{f235} = (3.85 \times 10^{-4} / \text{\AA}^3) (282 \times 10^{-24} \text{ cm}^2) (10^8 \text{ \AA/cm})^3 = 0.108 \text{ cm}^{-1}$$

$$\phi = 1.1 \times 10^{13} / \text{cm}^2 \text{ sec}$$

The σ_{f235} used was the Wigner-Wilkins spectrum averaged value given by LEOPARD. Using these parameters, the solution for $X(t)$ becomes:

$$X(t) = 0.0705 \times 10^{-15} [1 - e^{-.92t}] + 3.35 \times 10^{15} [0.571 e^{-.182t} - e^{-.104t}] + 1.43 \times 10^{15}$$

where the units of time are hours, and X is in $\#/\text{cm}^3$.

Now the reactivity ρ is defined (Reference 3)

$$\rho = \frac{\Sigma_{ax} / \Sigma f}{\nu p \epsilon} = \frac{-X \sigma_{ax} / \Sigma f}{\nu p \epsilon}$$

From LEOPARD, $p = 0.75$. Also $\nu = 2.44$ and $\epsilon = 1.0$ were assumed.

The resulting time dependent behavior of ρ as xenon builds-up is shown in Figure 10 and labeled "theoretical curve."

The data as obtained from the measurements of 19 November 1969 are also shown without the time shift on Figure 10, labeled "uncorrected data." It is clear that this curve falls far below the theoretical one. The results are very sensitive to the measurements of temperature made, since the reactivity is calculated in a summation process.

Thus, it was assumed that the temperature drops as recorded did not reflect the true build-up of xenon. Instead, each degree of ΔT was assumed to have been measured to be an additive constant $\delta/3$ less than its true value (e.g. a ΔT of 3 degrees was in reality a ΔT of $(3+\delta)$ degrees). The ΔP power measurements were assumed correct. Using δ as an unknown, the total build-up of xenon was calculated and set to equal the theoretical value, thus yielding one equation in the unknown δ :

$$\left\{ \begin{array}{l} t=40 \\ \sum \\ t=0 \end{array} \right\} \Delta \rho = \underbrace{\sum_{t=0}^{t=40} (\Delta T * \frac{\Delta \rho}{\Delta T})}_{\text{theoretical}} + \sum_{t=0}^{t=40} \left(\frac{\Delta T}{3} * \frac{\Delta \rho}{\Delta T} * \delta \right) + \sum_{t=0}^{t=40} (\Delta P * \frac{\Delta \rho}{\Delta P} + \$0.22)$$

This yields a value: $\delta = 2.27^\circ\text{F}$.

Thus, the ΔT recorded on 19 November 1969 were modified:

$$\Delta T' = \Delta T + \left(\frac{\Delta T}{3} \right) \delta$$

and the data corrected accordingly. The resulting curve is shown in Figure 10, labeled " δ -corrected data". It appears to agree well with the theoretical curve.

The equilibrium xenon is calculated from the theoretical curve to be -2.06 percent or -\$2.82. The δ -corrected curve predicts an equilibrium value of -\$2.8.

III

III. CONCLUSIONS

The core physics tests performed in November 1969 on Core 2 of the MH-1A have provided a great deal of useful information. They demonstrated the enormous time savings which result from the use of a reactivity computer in rod latch verification, stuck rod margin measurement, control rod calibration, and temperature coefficient measurement. They also showed that the reactor operators and data takers must be meticulous and conscientious in the performance of the tests and in recording data. Some of the data gathered in these tests did not provide the information which it should have. This is due to many factors; poorly worded procedures, failure to record required data, and general inexperience in the performance of core physics tests. On the basis of these tests the procedural problems can be cleared up prior to the next tests. The failure to record required data can be taken care of by better instruction and orientation of operating personnel. The problem of inexperience is not an easy one to overcome, due to the continual changeover of plant and program personnel. It definitely illustrates the requirement for the presence of an experienced nuclear plant test engineer in addition to the regular plant operating and management personnel.

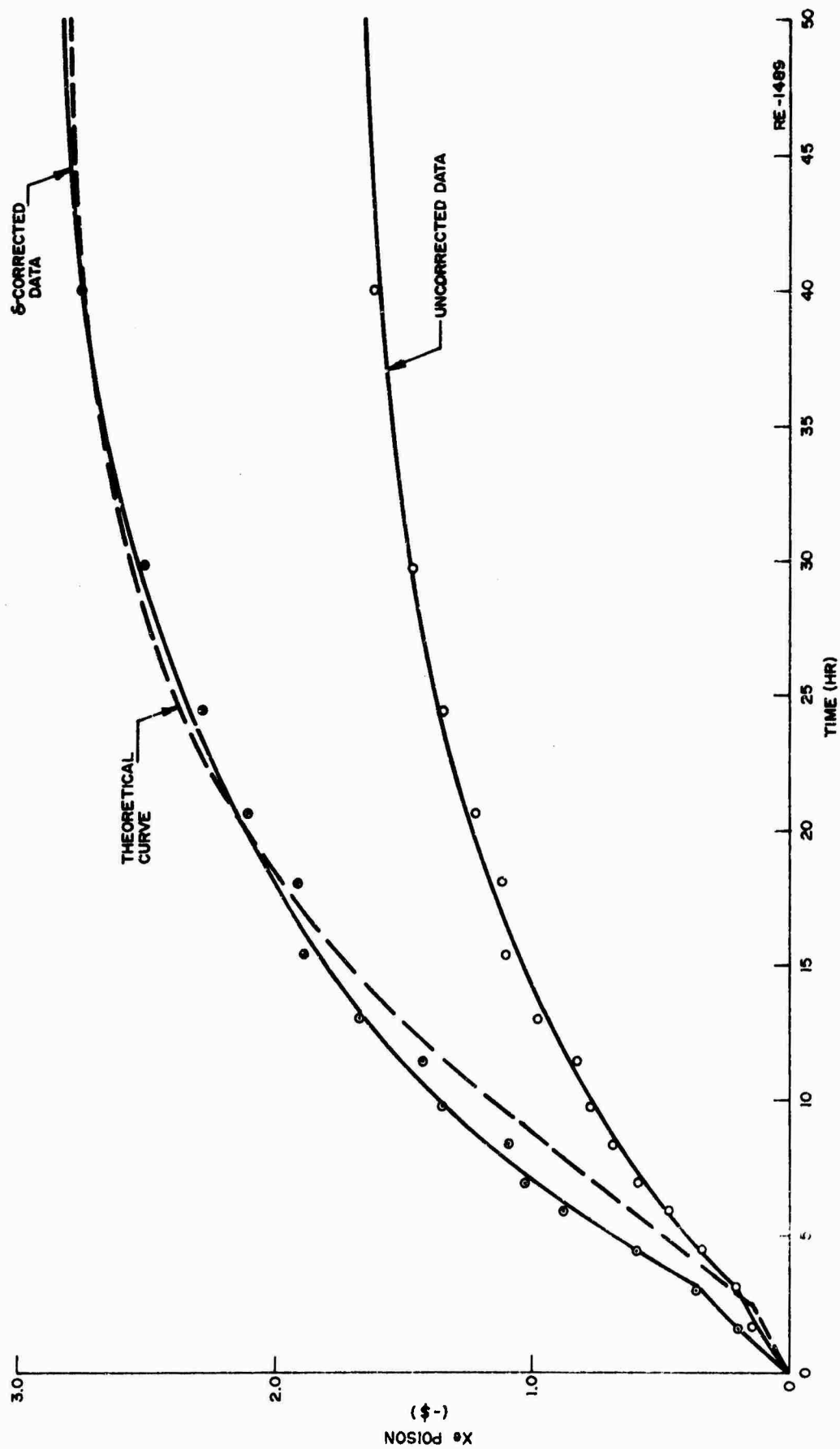


FIGURE 10. XENON BUILD-UP (CORRECTED DATA)

Table XII compares the present results with those of previous measurements and those expected from theoretical calculations. The agreement of present results with those based on previous experience or theory appear satisfactory.

Even though some of the tests provided poor results, the entire test has resulted in a better understanding of the MH-1A and its Nuclear performance.

TABLE XII
SUMMARY COMPARISON

	<u>Experimental</u>	<u>Theoretical (2)</u>	<u>Previous Core (1)</u>
Temperature coefficient (68°F)	$-0.81 \times 10^{-4}/^{\circ}\text{F}$	$-0.33 \times 10^{-4}/^{\circ}\text{F}$	$-0.3 \times 10^{-4}/^{\circ}\text{F}$
(490°F)	$-2.45 \times 10^{-4}/^{\circ}\text{F}$	$-2.7 \times 10^{-4}/^{\circ}\text{F}$	$-2.95 \times 10^{-4}/^{\circ}\text{F}$
Power coefficient	$-2.95 \times 10^{-4}/\text{MWT}$	$-2.1 \times 10^{-4}/\text{MWT}$	$-2.01 \times 10^{-4}/\text{MWT}$
Temperature defect	6.47% $\Delta \rho$	4.8% $\Delta \rho$	6.4% $\Delta \rho$
Equilibrium xenon	-1.4% $\Delta \rho$	-2.1% $\Delta \rho$	-2.0% $\Delta \rho$
Critical bank height (68°F)	11.48 inches (@ 150°F)	11.18 inches (@68°F)	11.3 inches (@100°F)

REFERENCES

1. Engineering Support Study: MH-1A Core Physics Test Results, 4 October 1968.
2. MH-1A Final Design Report, Nuclear Analysis MND-3238, September 1965.
3. Lamarsh, John R., Introduction to Nuclear Reactor Theory, Addison-Wesley Publishing Co., 1966.
4. LEOPARD Program output of 13 Feb 1970 for BOL spectrum @ 4.36% enrichment and hot.
5. MH-1A Refueling, ED-6923, October 1969.